Supporting Information for

A ^{18}F-labeled saxitoxin derivative for *in vivo* PET-MRI imaging of voltage-gated sodium channel expression following nerve injury

Aileen Hoehne,[+] Deepak Behera,[+] William H. Parsons,[+] Michelle L. James, Bin Shen, Preeti Borgohain, Deepika Bodapati, Archana Prabhakar, Sanjiv S. Gambhir, David C. Yeomans, Sandip Biswal,* Frederick T. Chin,* J. Du Bois*

CONTENTS

EXPERIMENTAL S3
Synthetic Procedures and Characterization Data S3
General S3
Synthesis of [^{19}F]STX S3
Cell Culture and Electrophysiology S4
Radiosynthesis S5
General S5
Radiosynthesis of N-succinimidyl 4-[^{18}F]fluorobenzoate ([^{18}F]SFB) S6
Radiosynthesis of 6-(4-[^{18}F]fluorobenzamido)hexylcarbamoyl-saxitoxin ([^{18}F]STX) S6
Spared nerve injury model S7
Behavioral test for pain S7
Ex vivo determination of radiometabolites in rats S8
Biodistribution of [^{18}F]STX in rats and autoradiography of excised nerves S8
PET-MRI imaging S9
Image analysis S9
Autoradiography S9
PET/MRI S9
Statistical analysis S10
SUPPLEMENTARY FIGURES AND TABLES S11
Figure S1: 1H NMR of [^{19}F]STX. S11
Figure S2: Electrophysiology. S12
Figure S3: Radiochemistry. S13
Figure S4: Analytical HPLC chromatograms. S14
Figure S5: Behavioral tests. S15
Figure S6: *In vivo* radiotracer stability. S16
Figure S7: Experimental set-up for *ex vivo* studies. S17
Figure S8: Biodistribution of [^{18}F]STX in SNI rats without and with co-injection of [^{19}F]STX. S18
Figure S9: Composite PET-MRI images. S20
Table S1: Biodistribution. S21
SUPPLEMENTARY DISCUSSION S22
REFERENCES S13

EXPERIMENTAL

Synthetic Procedures and Characterization Data

Caution

Saxitoxin derivatives are expected to show similar toxicity and symptomatology to saxitoxin, tetrodotoxin, and other sodium channel blockers and should be handled with appropriate care for safety.[1]

General

All reagents were obtained commercially unless otherwise noted. **STX-NH_3^+** was synthesized according to the procedure of Andresen and Du Bois.[2] Semi-preparative high performance liquid chromatography (HPLC) was performed on a Varian ProStar model 210. Nuclear magnetic resonance (NMR) spectra were acquired on a Varian Inova spectrometer operating at 500 MHz for ^{1}H and are referenced internally according to residual solvent signals. Data for ^{1}H NMR are recorded as follows: chemical shift (δ, ppm), multiplicity (s, singlet; d, doublet; t, triplet; q, quartet; quint, quintet; m, multiplet; br, broad), integration, coupling constant (Hz). High-resolution mass spectra were obtained from the Vincent Coates Foundation Mass Spectrometry Laboratory at Stanford University.

Synthesis of [^{19}F]STX

To a solution of the heptafluorobutyrate salt of **STX-NH_3^+** (2.2 mg, 2.1 μmol) in 560 μL of a 1:3 mixture of pH 9.5 solution (0.1 M $NaHCO_3/Na_2CO_3$) and DMF was added 4-fluorobenzoic acid *N*-hydroxysuccinimide ester (**[^{19}F]SFB**, 1.7 mg, 6.2 μmol, 3.0 equiv). The solution was stirred for 2 h, then acidified with 30 μL of 1.0 M aqueous trifluoroacetic acid. The mixture was lyophilized to give a solid material that was purified by reverse phase HPLC (Silicycle AQ C18, 5 μm, 10 x 250 mm column, eluting with a gradient flow over 40 min of 15:85 MeCN/0.1% aqueous CF_3CO_2H → 35:65 MeCN/0.1% aqueous CF_3CO_2H, 254 nm UV detection). At a flow rate of 4 mL/min, **[^{19}F]STX** had a retention time of 19.6 min and was isolated following lyophylization as a white powder (1.4 mg, 87%): ^{1}H NMR (D_2O, 500 MHz) δ 7.75-7.72 (m, 2H), 7.21-7.18 (m, 2H), 4.68 (s, 1H), 4.21 (dd, 1H, *J* = 12.0, 9.5 Hz), 3.84 (dd, 1H, *J* = 12.0, 5.5 Hz), 3.78-3.74 (m, 2H), 3.54-3.49 (m, 1H), 3.34 (dd, 2H, *J* = 7.0, 7.0 Hz), 3.10-3.03 (m, 2H), 2.40-2.26 (m, 2H), 1.61-1.55 (m, 2H), 1.48-1.43 (m, 2H), 1.38-1.28 (m, 4H) ppm; HRMS (ES^+) calcd for $C_{23}H_{33}FN_8O_5$ 520.2558 found 521.2639 (MH^+).

The coupling reaction can also be performed with an excess of **STX-NH_3^+** (1.0 mg, 0.96 μmol, 4.0 equiv) and a limiting amount of **[^{19}F]SFB** (60 μg, 0.24 μmol). After 1 h of stirring, acidification of the reaction mixture and purification by reverse phase HPLC using the method described above gave **[^{19}F]STX** (0.16 mg, 88%). Unreacted **STX-NH_3^+** had a retention time of 4.5 min.

Cell Culture and Electrophysiology

Chinese hamster ovary (CHO) cell culture was performed as described previously.[2] Transfection with either a pZem228 vector containing the full-length cDNA coding for the α-subunit of rat $Na_V1.4$ ($rNa_V1.4$)[3] or a pcDNA3.1(+) vector containing the full-length cDNA coding for the α-subunit of human $Na_V1.5$ ($hNa_V1.5$)[4] was accomplished using the calcium phosphate precipitation method. Cotransfection with eGFP was used as a marker of transfection efficiency.

PC12 (pheochromocytoma 12) cell culture was performed as described previously.[5] For electrophysiological recordings involving differentiated PC12 cells, 100 ng/mL of nerve growth factor (NGF; BD Biosciences, Bedford, MA) was added 3–4 days prior to data collection.

Sodium currents were measured using the patch-clamp technique in the whole-cell configuration with an Axopatch-200b amplifier (Axon Instruments, Union City, CA), as previously described by Moran.[6] Borosilicate glass micropipettes (Sutter Instruments, Novato, CA) were fire-polished to a tip diameter yielding a resistance of 1.5–3.0 MΩ in the working solutions. For experiments with CHO cells, the pipette was filled with (in mM): NaF 40, EDTA 1, HEPES 20, CsCl 125, and the pH was adjusted to 7.4 with solid CsOH. The external solution had the following composition (in mM): NaCl 160, $CaCl_2$ 2, HEPES 20, and the pH was adjusted to 7.4 with solid CsOH. For experiments with PC12 cells, pipettes were filled with (in mM): CsCl 140, KCl 1, EGTA 1, HEPES 10, and the pH was adjusted to 7.2 with solid CsOH. The external solution had the following composition (in mM): NaCl 140, $CaCl_2$ 1, HEPES 10, and the pH was adjusted to 7.4 with solid CsOH.[7]

The output of the patch-clamp amplifier was filtered with a built-in low-pass, four-pole Bessel filter having a cutoff frequency of 10 kHz and sampled at 100 kHz. The membrane was kept at a holding potential of –100 mV. Pulse stimulation and data acquisition used 16 bit D-A and A-D converters (Axon Instruments Digidata 1322A) controlled with the PClamp software (Axon Instruments). Leak currents were subtracted using a standard P/4 protocol of the same polarity. Access resistance was always <4 MΩ and the cell capacitance was between 4 and 20 pF, as measured by the compensating circuit of the amplifier. The series resistance was usually compensated between 80% and 85%. All measurements were done at room temperature (20–22 °C).

Recordings were made at least 5 min after establishing the whole-cell and voltage-clamp configuration to allow for stabilization of the voltage-dependent properties of the channels. Currents were elicited by 10 ms step depolarizations from a holding potential of –100 to 0 mV. Solutions of **STX** and **[^{19}F]STX** were prepared by serial dilution with external solution and stored at 4 °C. Current measurements were recorded under continuous perfusion, controlled manually by syringe addition. Data were normalized to control currents, plotted against toxin concentration and analyzed using custom software developed in the Igor environment (Wavemetrics). Data were fitted to Langmuir isotherms to elicit IC50 values and expressed as mean ± SE.

Radiosynthesis

General

All chemicals unless otherwise stated were commercially available and used without further purification. Ethyl 4-*N*,*N*,*N*-trimethylammoniumbenzoate trifluoromethanesulfonate was synthesized according to a literature procedure.[8] Analytical high-performance liquid chromatography (HPLC) analyses were performed on a PeakSimple chromatography data system equipped with a LabAlliance Pump Series III, a LabAlliance UV absorbance detector Model 500 and a model 105S single-channel radiation detector (Carroll & Ramsey Associates) using a Phenomenex Gemini C18 column (250 × 4.6 mm, 5 µm) and isocratic conditions (25% CH_3CN in H_2O + 0.1% TFA; 1.0 mL/min) with UV chromatograms recorded at 214 nm or on an Agilent 1200 Series HPLC system with ChemStation software (version B.04.02) equipped with a quaternary pump, UV diode array detector and model 105S single-channel radiation detector (Carroll & Ramsey Associates) using a Phenomenex Gemini C18 column (250 × 4.6 mm, 5 µm) and gradient conditions (A: H_2O + 0.1% TFA, B: CH_3CN + 0.1% TFA; 0-12 min 10-40% B, 12-13 min 40-95% B, 13-18 min 95% B, 18-18 min 95-10% B, 19-25 min 10% B; 1.0 mL/min) with UV chromatograms recorded at 214 and 254 nm. The identity of the ^{18}F-labeled products was confirmed by comparison with the HPLC retention time of their non-radioactive reference molecule or by co-injection. Semi-preparative HPLC purifications were carried out on a Dionex Ultimate 3000 system with Chromeleon 6.80 software equipped with UV diode array and model 105S single-channel radiation detector (Carroll & Ramsey Associates) using a Phenomenex Luna C18 column (250 × 10 mm, 5 µm) and gradient conditions (A: H_2O + 0.1% TFA, B: CH_3CN + 0.1% TFA; 0-30 min 10-35% B, 30-31 min 35-95% B, 31-36 min 95% B, 36-37 min 95-10% B, 37-40 min 10% B; 3.0 mL/min).

Radiosynthesis of N-succinimidyl 4-[^{18}F]fluorobenzoate ([^{18}F]SFB)

For the radiosynthesis of **[^{18}F]SFB**, the manual method described by Tang et al.[9] was semi-automated using a GE Tracerlab FX-FN module (**Figure S3**).

Briefly, no-carrier added [^{18}F]fluoride was produced via the ^{18}O(p,n)^{18}F nuclear reaction by irradiation of enriched [^{18}O]H_2O in a PETtrace cyclotron (General Electric). [^{18}F]Fluoride was trapped on an anion-exchange resin cartridge (Macherey-Nagel Chromafix 30-PS-HCO_3 pre-conditioned with 1 mL EtOH, 1 mL H_2O and then blown dry). The cartridge was eluted with a solution of Kryptofix K2.2.2. (15 mg) and potassium carbonate (3 mg) in H_2O (0.1 mL) and CH_3CN (0.9 mL). Following drying, ethyl 4-*N*,*N*,*N*-trimethylammoniumbenzoate trifluoromethanesulfonate (3.0 mg in 1.0 mL dry CH_3CN) was added to the K[^{18}F]F/K2.2.2. complex, and the mixture was heated for 10 min at 90 °C to yield ethyl 4-[^{18}F]fluorobenzoate. After cooling the reaction mixture to roomp temperature, tetrapropylammonium hydroxide (50 μL of 1.0 M aqueous solution in 1.0 mL CH_3CN) was added and heated for 3 min at 120 °C to give 4-[^{18}F]fluorobenzoic acid as the tetrapropylammonium salt. The reaction mixture was cooled to room temperature and solvents were removed under reduced pressure and a stream of helium at 65-88 °C. The dried tetrapropylammonium 4-[^{18}F]fluorobenzoate was re-dissolved in 1.5 mL dry CH_3CN and this solution was transferred into a 10 mL-V-vial containing *O*-(*N*-succinimidyl)-1,1,3,3-tetramethyl uranium tetrafluoroborate (TSTU) (10 mg). The V-vial was transferred to a heating block set at 90 °C. After 5 min incubation, the V-vial was removed from the heating block and the reaction mixture containing **[^{18}F]SFB** was diluted with 8 mL 5% glacial acetic acid in H_2O. This solution was transferred into a large-volume collection vial containing 12 mL H_2O. The content of the collection vial was then passed through a Waters SepPak C18 Plus cartridge (pre-conditioned with 5 mL EtOH, 10 mL H_2O) in order to trap the **[^{18}F]SFB**. The cartridge was washed once with 10 mL 10% CH_3CN in H_2O, blown dry with helium and then eluted with dry acetonitrile (3 mL) through a Merck Lichrolut SCX cartridge (pre-conditioned with 5 mL 0.1 N HCl, 20 mL H_2O, 5 mL acetonitrile) and a Varian Na_2SO_4 cartridge (2.2 g) into a 5 mL-V-vial with stirrer bar. Finally, the solvent was evaporated at 60 °C under vacuum and a stream of helium to yield the desired product, as confirmed by comparison to the HPLC retention time of nonradioactive **[^{19}F]SFB**.

Radiosynthesis of 6-(4-[^{18}F]fluorobenzamido)hexylcarbamoyl-saxitoxin (**[^{18}F]STX)**

The tris-heptafluorobutyrate salt of 6-aminohexylcarbamoyl-saxitoxin (**STX-NH_3^+**, 400-500 μg) was dissolved in 50 μL 0.1 M sodium carbonate buffer (pH 9.5) and 150 μL DMF. The solution was added to a vial containing dried **[^{18}F]SFB**. The reaction mixture was stirred at 50 °C for 30-40 min. Following this time, the mixture was diluted with H_2O

+ 0.1% trifluoroacetic acid injected onto a semipreparative HPLC column. The fraction corresponding to the peak of the desired product (retention time ~24.8 min) was collected. Solvents were evaporated under reduced pressure and the product was re-constituted in PBS. The identity of the formulated product was confirmed by comparison to the HPLC retention time of nonradioactive **[^{19}F]STX** and co-injection of both radioactive and nonradioactive material.

Spared nerve injury model

All experimental procedures involving animals were performed under humane conditions following approval from the Stanford Administrative Panel on Laboratory Animal Care (APLAC). Animals had access to food and H_2O ad libitum and were kept under a 12 h light/dark cycle. Thirty adult male Sprague-Dawley rats (200-250 g) underwent a left Spared Nerve Injury (SNI) procedure, which creates a well-characterized rat neuropathic pain model.[10] Briefly, animals were anesthetized with inhalational 2-3% isoflurane and placed on a warming bed. The posterolateral aspect of the left thigh was shaved and prepared aseptically for surgery. Following a longitudinal skin incision, the left sciatic nerve was identified, exposed and followed distally until its trifurcation into the tibial, common peroneal and sural nerves. A ligation and transection of the tibial and common peroneal nerves was done with cautious sparing of the sural nerve. The muscle layer was closed with absorbable interrupted sutures and the skin was apposed with staples. After recovery from anesthesia, animals were returned to their cages and allowed free access to food and water. The staples were removed 5 days after the surgery. This procedure provokes a chronic mechanical and thermal hypersensitivity; onset of symptoms occurs by 24 hours, and lasts several months. The right hind limb was used as control. In addition, three rats underwent a sham operation which comprised of a similar surgery but without any nerve ligation or transection. The rats were allowed 4 weeks to heal and develop pain.

Behavioral test for pain

Pain sensation was ascertained the day before imaging by behavioral testing for mechanical allodynia using von-Frey's filaments. Briefly, the animals were acclimatized on an elevated wire-mesh floor for two hours each day for four days prior to testing and an hour just before testing. Filaments of serially increasing stiffness were applied to the lateral part of plantar aspect of both hind paws through the mesh floor and pressed until they bent. A brisk withdrawal of the paw off the mesh floor was considered a positive response. In the absence of a positive response, the next filament with greater stiffness was used. A positive response was confirmed by repeating the test with the same filament till three consecutive responses were positive. The data thus collected was

analyzed using the PsychoFit software (source: http://psych.colorado.edu/~lharvey/html/software.html), which calculates the 50% withdrawal threshold in log filament stiffness units. The threshold is defined as the stimulus intensity at which the withdrawal is detected 50% of the time.

Ex vivo determination of radiometabolites in rats

Two SNI rats were administered **[^{18}F]STX** (1000 µCi/37 MBq in 700 µL of 0.9% saline solution) via tail vein injection. Rats were monitored for signs of toxicity such as respiratory distress and abnormal changes in heart rate. Urine (300 µL) was diluted with 500 µL ice-cold acetonitrile and centrifuged (9,400 *g*, 4 min). An aliquot of each supernatant (100 µL) was analyzed via the same HPLC method used for quality control of **[^{18}F]STX**. The percent ratio of intact **[^{18}F]STX** (tR = 11.3 min) on the HPLC chromatogram was calculated as % = (peak area for **[^{18}F]STX**/total peak area)*100.

Biodistribution of [^{18}F]STX in rats and autoradiography of excised nerves

Rats were administered **[^{18}F]STX** (200-500 µCi/7-19 MBq in 200-800 µL of 0.9% saline solution) via tail vein injection. In blocking studies, 9 nmol **[^{19}F]STX** in 100 uL PBS was co-administrated with the tracer. Animals were then euthanized by bilateral thoracotomy under anesthesia at 5, 10, 15, 30, 45, and 60 min after injection of tracer (n = 3 for each time point). Blood samples (200-1000 µL) were collected via cardiac puncture immediately prior to euthanizing. Tissue samples (heart, left and right nerve, surgical wound, whole brain, kidney, liver, lung, muscle, small intestine, spleen, bone) were removed quickly following euthanasia and placed in pre-weighed test tubes. The vertebral column was isolated and cut into cervical, upper thoracic, lower thoracic and lumbar sections according to corresponding vertebrae. The spinal cord parts were then flushed out from within the vertebral column with PBS and placed in pre-weighed test tubes. Standard solutions of the tracer were prepared by diluting approximately 100 µCi tracer in 100 mL water, of which 1 mL aliquots were used for reference counting.

The test tubes containing tissue samples were weighed and radioactivity was measured by an automated gamma counter (Cobra Model 5002, Packard, Meriden, CT) along with the standard solutions. The percentage of injected dose per gram of tissue (%ID/g) was calculated after decay-correction.

Ex vivo autoradiography was performed on segments of left (injured) and right (uninjured) sciatic nerves harvested from the thighs of all rats at the aforementioned time points. After excision, the nerves were immediately exposed on a phosphor screen (medium MultiSensitive Phosphor Screen; PerkinElmer) overnight. The screen was imaged using a variable-mode imager (Typhoon 9410; GE Healthcare).

PET-MRI imaging

For PET-MRI, animals (n = 5) were anesthetized with humidified, oxygen enriched 2-3% isoflurane (inhalation) and rigidly secured in a transportable holder to minimize motion while being transferred between the PET and MRI scanners. Fiducial markers made with diluted radioactive solution (30 µCi/mL) were utilized for assistance in PET and MRI image co-registration. For PET scanning, each animal was given approximately 500 µCi of **[^{18}F]STX** intravenously. Beginning 10 minutes after injection, a static PET image of the thighs was acquired for 10 minutes (microPET R4; Siemens Medical Solutions). This was followed by T1-weighted fast spin echo images of the thighs (TR, 800ms; TE, 7.7 ms; slice thickness, 1 mm; in plane resolution, 234 µm) obtained using a 7T small-animal MRI (a self-shielded 30-cm-bore 7-T magnet [Varian] with a 9-cm-bore gradient insert [Resonance Research Inc.] using EXCITE2 electronics and the supporting LX11 platform [GE Healthcare]).

Image analysis

Autoradiography

The autoradiography images were analyzed using ImageJ software *(source:* http://rsbweb.nih.gov/ij/*)*. [11] The maximum signal in each left (injured) nerve was normalized to the average signal in three randomly drawn regions of interest within the same nerve, carefully avoiding the site of injury (neuroma). The average signal in the corresponding right (uninjured) nerve was also calculated from three random regions of interest for each rat as an internal control.

PET/MRI

The PET and MRI scans were co-registered using Inveon Research Workplace (IRW; Siemens Healthcare) image analysis software. The MR images were used to define the anatomic location of the sciatic nerves and regions of interest (ROIs) were placed on 5 consecutive transaxial slices covering the site of injury (neuroma around the site of ligation and transection) on the left nerves and corresponding regions on the right nerve. Radioactivity counts were then recorded from within the ROIs in the fused PET images. The maximum signals from all ROIs on a particular nerve were averaged to derive an average maximum signal for that nerve. The nerve signal was normalized to the average signal from adjacent muscle derived from cylindrical ROIs placed medial to the nerves.

Statistical analysis

Statistical analysis was done using IBM SPSS Statistical Analysis software (version 19) using two tailed paired t-tests to compare behavioral and PET data from injured and uninjured sides. Univariate Analysis of Variance was used to compare multiple means, as well as to determine significance of effect of blocking followed by Turkey's post hoc analysis if significance was achieved. One-way between subjects ANOVA with trend analysis was used to determine whether **[^{18}F]STX** uptake at the site of injury (neuroma) changed with time after injection.

SUPPLEMENTARY FIGURES AND TABLES

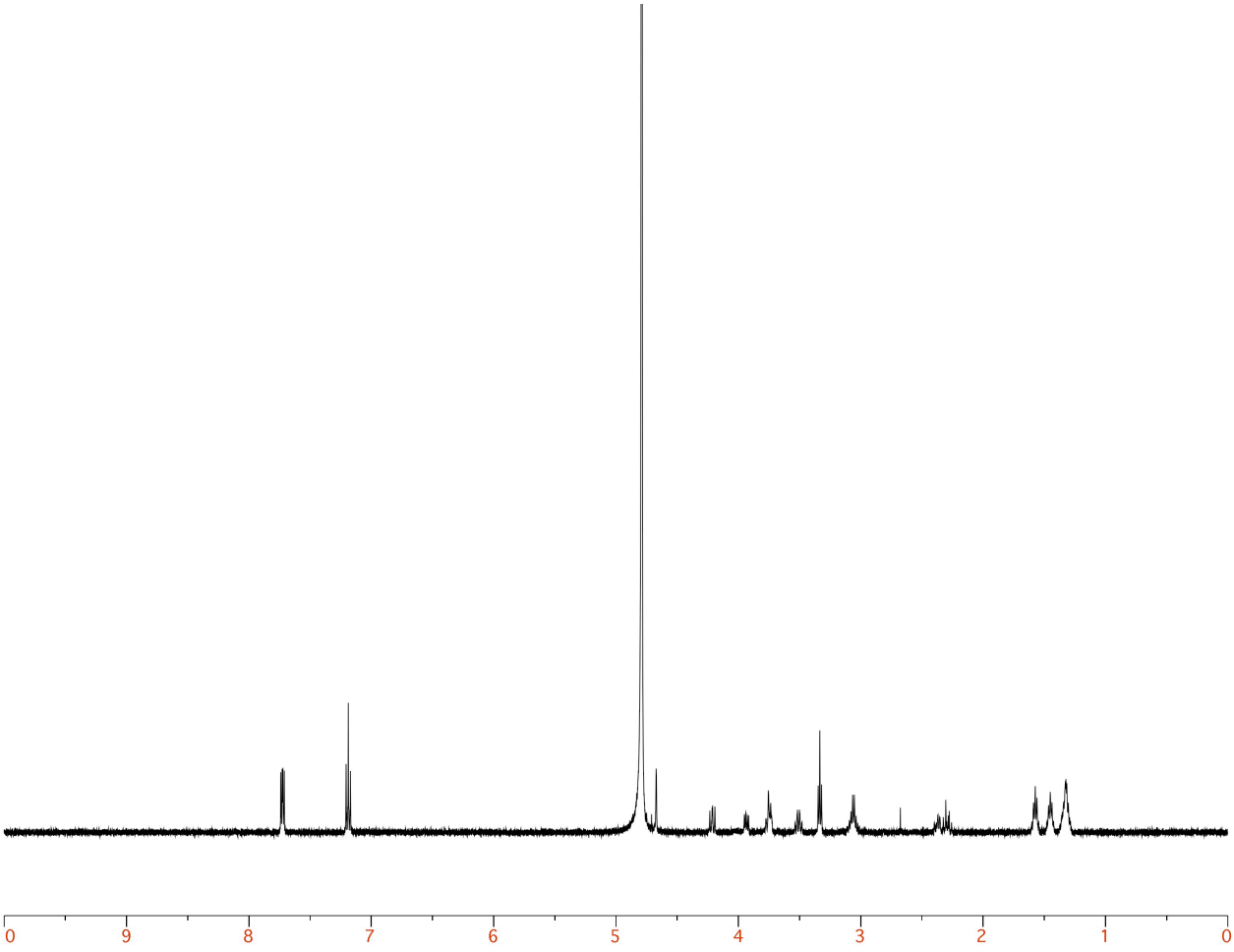

Figure S1: 1H NMR of [^{19}F]STX. ^{1}H NMR spectrum of synthesized **[^{19}F]STX** in D_2O (referenced to 4.79 ppm).

(a)

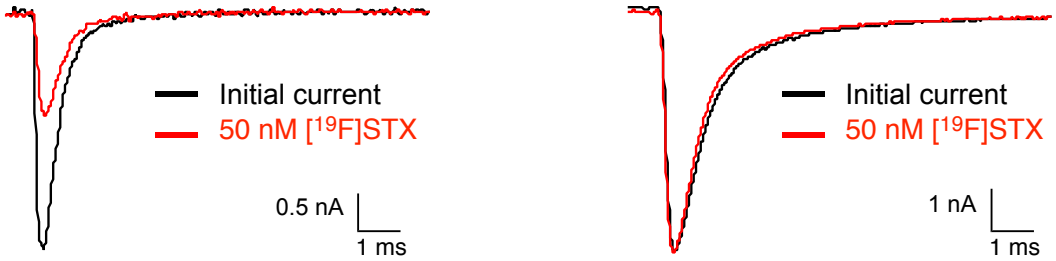

$Na_V1.4$ in CHO **$Na_V1.5$ in CHO**

(b)

	IC_{50} for [^{19}F]STX	**IC_{50} for STX**
rNa_V1.4 in CHO	46 ± 7 nM[a]	2.9 ± 0.1 nM[a]
hNa_V1.5 in CHO	1400 ± 170 nM	256 ± 20 nM
PC12 (Na_V1.2, Na_V1.7)	10.6 ± 0.6 nM	2.1 ± 0.2 nM[b]

[a] Value reported in Ref. 2.

[b] Value reported in Ref. 5.

Figure S2: Electrophysiology. (a) Whole-cell recordings from CHO cells heterologously expressing $Na_V1.4$ and $Na_V1.5$, respectively, before and after the addition of 50 nM **[^{19}F]STX**; currents were elicited by a 10 ms voltage step to 0 mV from a holding potential of -100 mV. (b) Compiled IC_{50} values for **[^{19}F]STX** and **STX** against several isoforms of Na_V.

(a)

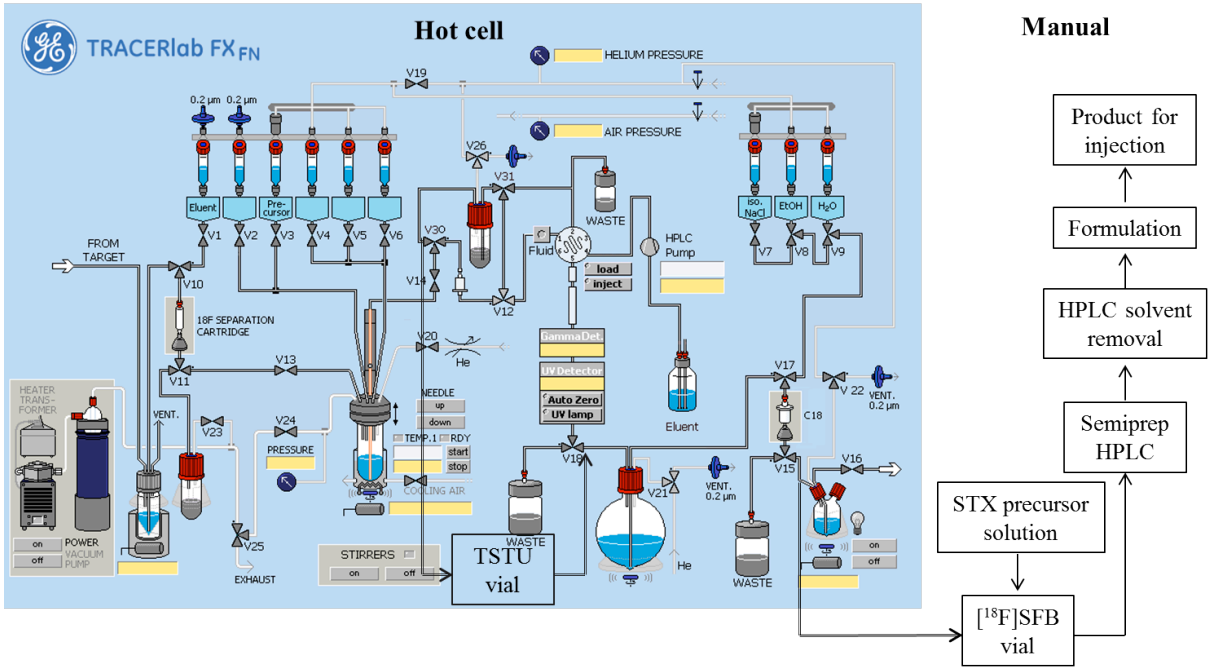

(b)

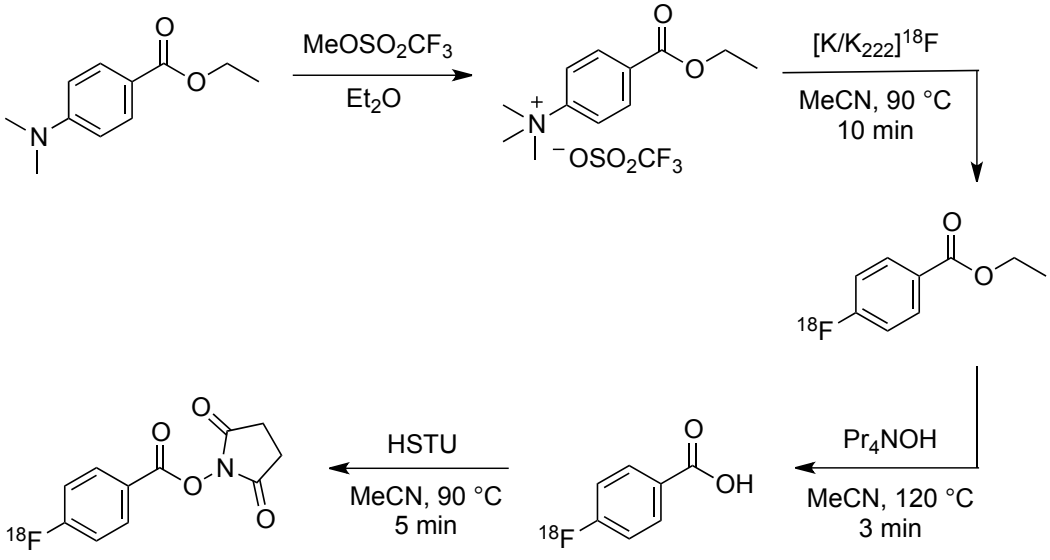

Figure S3: Radiochemistry. a) **[^{18}F]SFB** is synthesized in a GE TRACERlab FX-FN module located in a hot cell and subsequently coupled with 6-aminohexylcarbamoyl-saxitoxin in a lead-shielded fume hood; (b) Scheme for synthesis of **[^{18}F]SFB**.

(a)

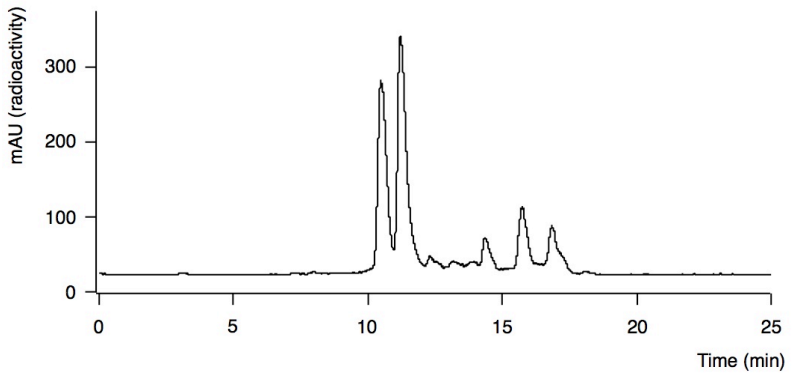

(b)

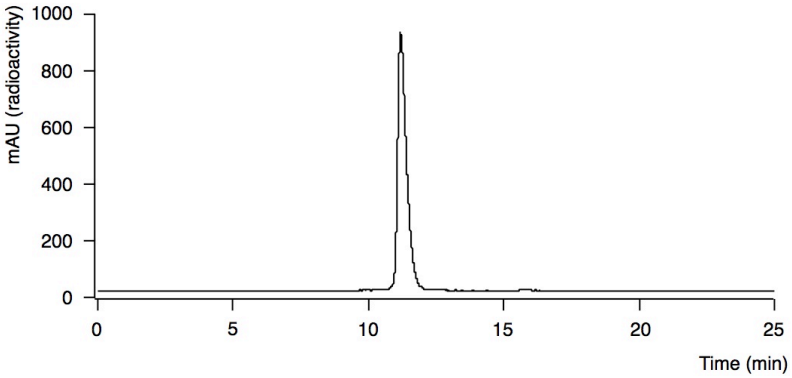

(c)

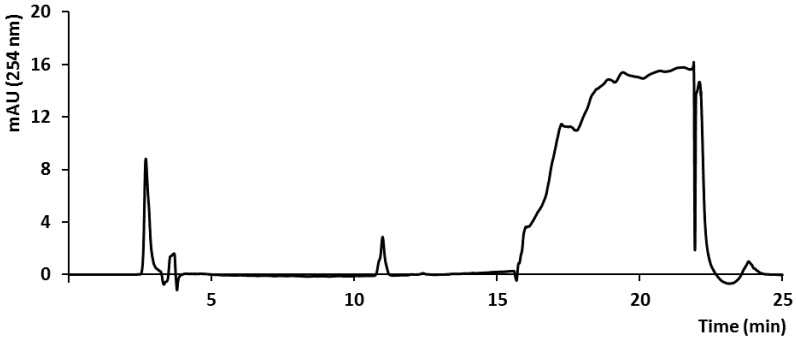

Figure S4: Analytical HPLC chromatograms. (a) Analytical HPLC trace of radioactivity for the crude reaction mixture before semi-prep HPLC purification; (b) Analytical HPLC trace of radioactivity for **[^{18}F]STX,** following purification and formulation in PBS. (c) HPLC UV trace for co-injection of purified and formulated **[^{18}F]STX** with **[^{19}F]STX,**

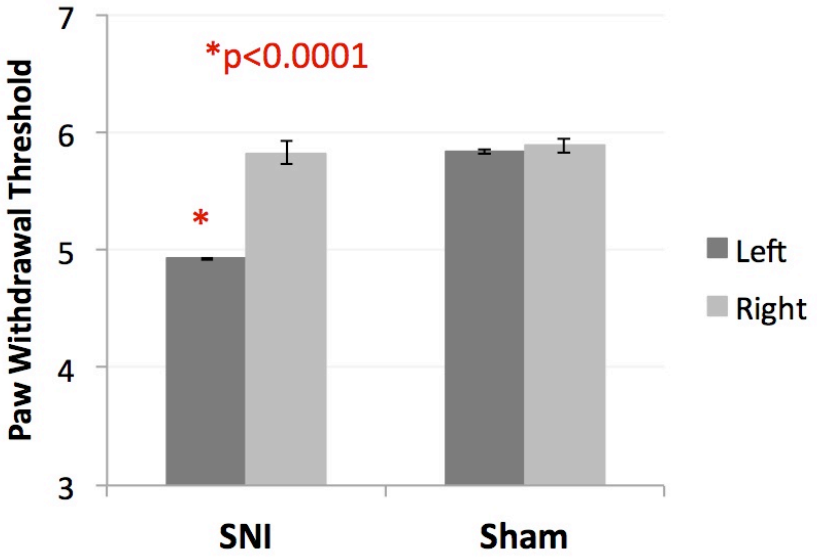

Figure S5: Behavioral tests. Behaviorial test for allodynia using von Frey filaments shows lower threshold for paw withdrawal in the injured left nerve in SNI animals, indicating presence of pain.

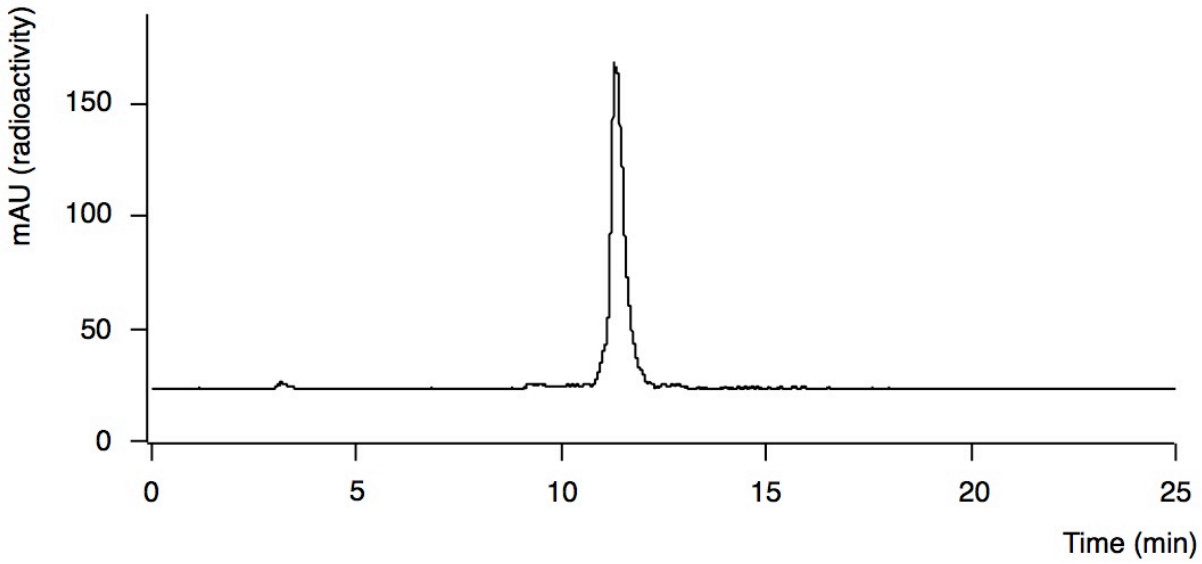

Figure S6: *In vivo* radiotracer stability. Analytical HPLC trace of urine collected from animal injected with **[^{18}F]STX** and sacrificed after 60 minutes. The peak eluting at 11.4 minutes, identical to the retention time of the radiotracer, represents 97% of the total area for the radioactive signal.

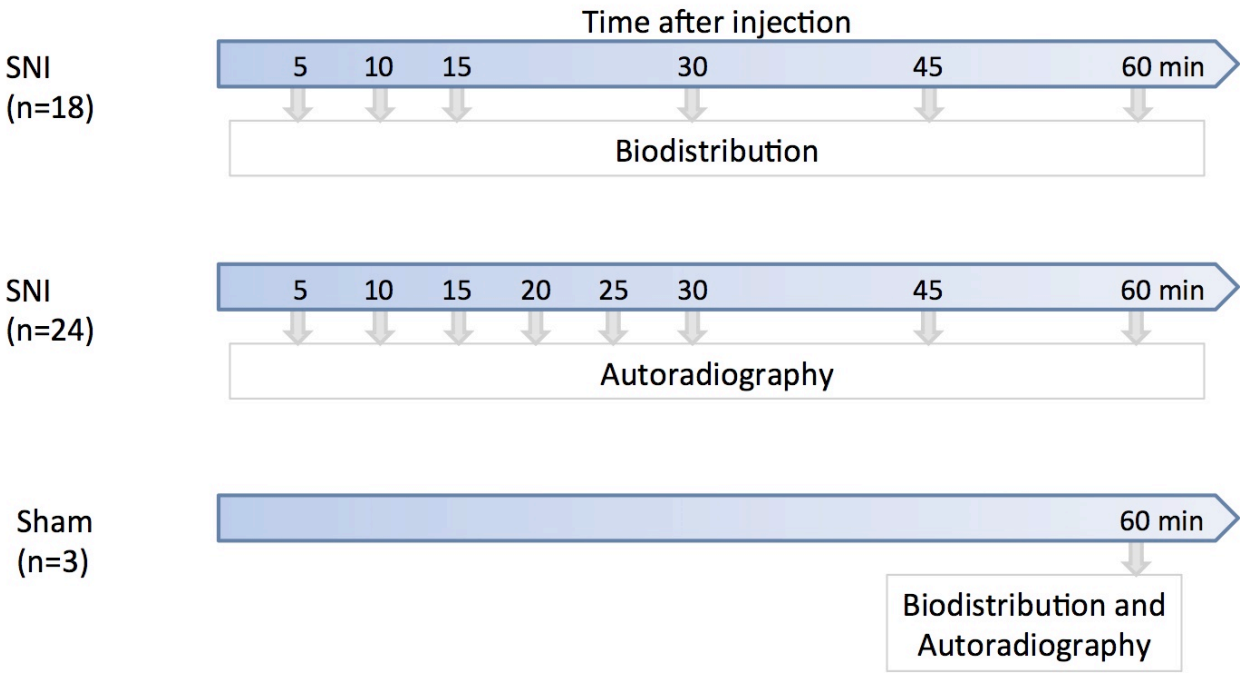

Figure S7: Experimental set-up for *ex vivo* studies. A graphical depiction of the experimental design for the biodistribution and autoradiography studies.

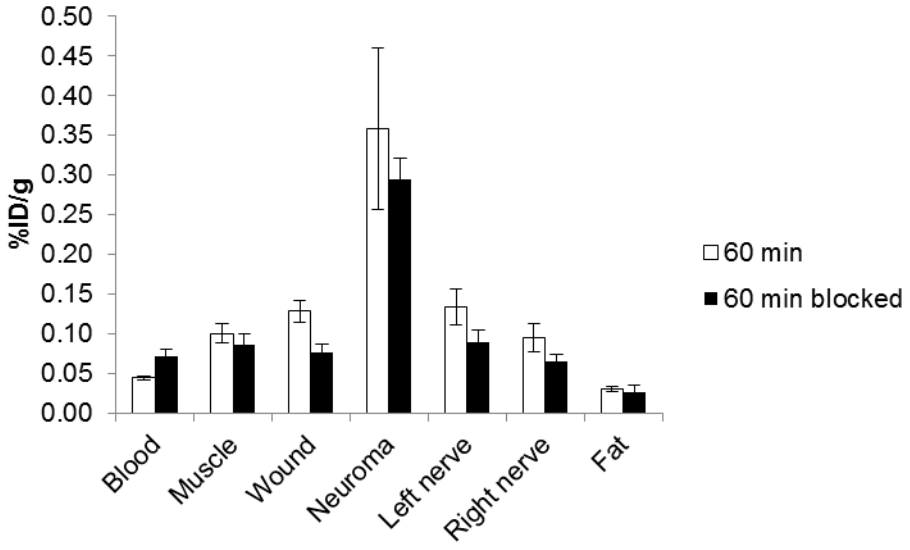

Figure S8: Biodistribution of [^{18}F]STX in SNI rats without and with co-injection of [^{19}F]STX. No significant effects of blocking were observed with Univariate Analysis of Variance. Data acquired at 60 min post-injection (n = 3 per group, error bars represent standard errors).

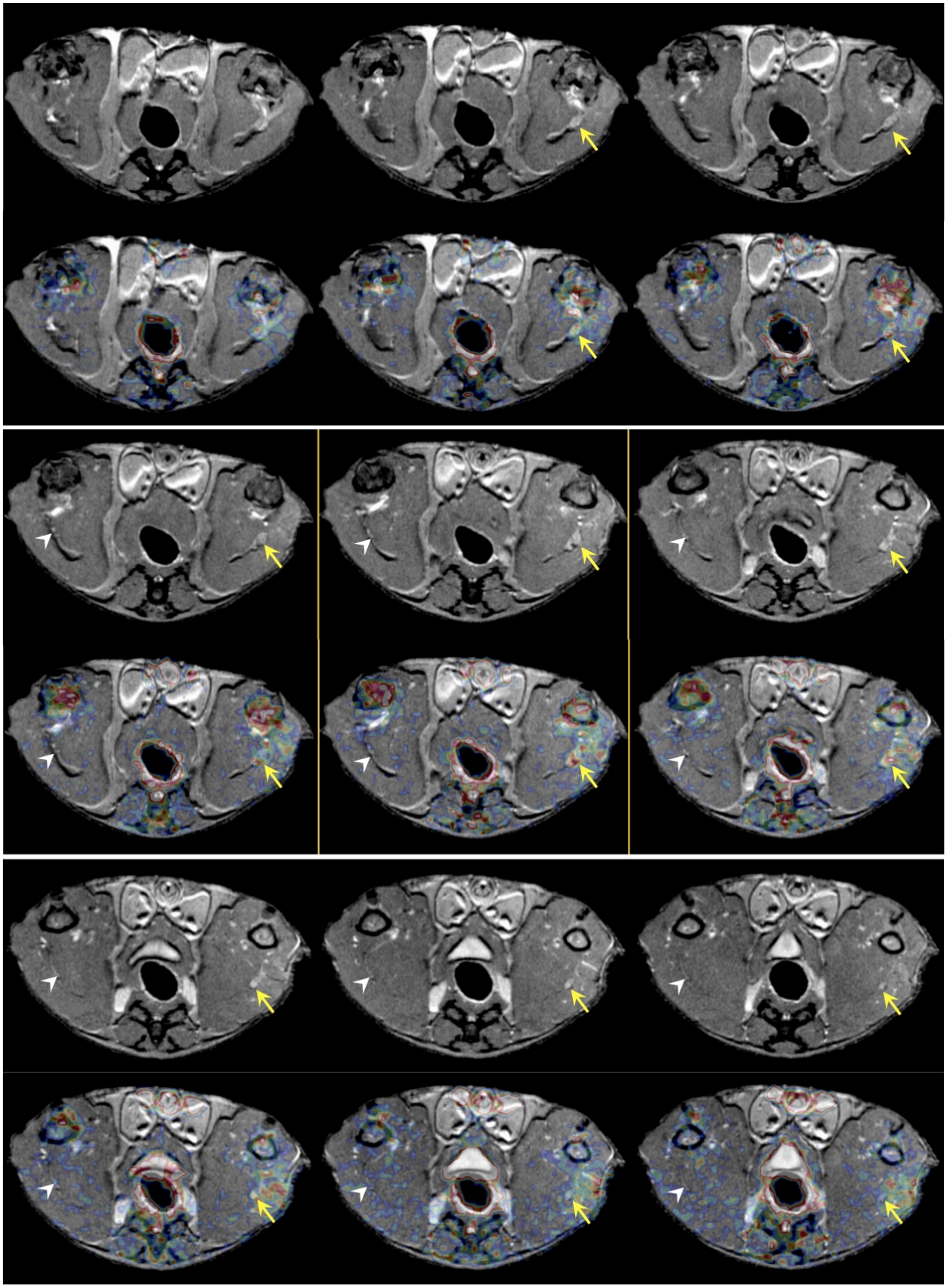

Figure S9: Composite PET-MRI images. Axial images of MRI (upper rows) and corresponding fused PET-MRI (lower rows) through four contiguous slices above and below the representative slices shown in Figure 6 (highlighted). The slices are in a caudal-to-cranial direction. The left injured nerve (yellow arrows) shows **[^{18}F]STX** uptake only in the neuroma. The right uninjured nerve (white arrowheads) shows no tracer uptake throughout.

Tissue	5 min	10 min	15 min	30 min*	45 min	60 min
Blood	0.19 *0.02*	0.15 *0.01*	0.10 *0.00*	0.08 *0.01*	0.06 *0.00*	0.05 *0.01*
Brain	0.01 *0.00*	0.01 *0.00*	0.01 *0.00*	0.01 *0.00*	0.01 *0.00*	0.01 *0.00*
Heart	1.79 *0.26*	1.55 *0.33*	1.60 *0.30*	0.97 *0.05*	0.95 *0.34*	0.83 *0.17*
Intestine (Small)	1.49 *0.08*	1.46 *0.22*	1.46 *0.43*	1.14 *0.15*	1.02 *0.86*	1.23 *0.36*
Kidney	1.79 *0.38*	1.17 *0.25*	1.11 *0.13*	1.47 *0.11*	1.40 *0.51*	1.90 *0.53*
Liver	0.64 *0.06*	0.80 *0.25*	0.97 *0.25*	0.75 *0.04*	1.42 *0.94*	1.35 *0.55*
Lung	0.93 *0.11*	0.67 *0.09*	0.67 *0.04*	0.54 *0.02*	0.45 *0.12*	0.43 *0.15*
Muscle	0.07 *0.00*	0.09 *0.02*	0.09 *0.01*	0.10 *0.02*	0.09 *0.02*	0.08 0.01
Spinal cord – cervical section	0.01 *0.00*	0.01 *0.00*	0.01 *0.00*	0.01 *0.00*	0.01 *0.01*	0.01 *0.00*
Spinal cord – upper thoracic section	0.01 *0.00*	0.02 *0.01*	0.01 *0.00*	0.01 *0.00*	0.01 *0.00*	0.01 *0.00*
Spinal cord – lower thoracic section	0.01 *0.00*	0.02 *0.01*	0.01 *0.00*	0.01 *0.00*	0.01 *0.00*	0.01 *0.00*
Spinal cord – lumbar section	0.02 *0.01*	0.01 *0.01*	0.02 *0.00*	0.02 *0.00*	0.02 *0.01*	0.01 *0.00*
Spleen	0.61 *0.16*	0.67 *0.24*	0.47 *0.21*	0.51 *0.13*	0.40 *0.06*	0.38 *0.11*
Bone (Femur)	0.11 *0.01*	0.11 *0.01*	0.10 *0.01*	0.07 *0.01*	0.08 *0.02*	0.07 *0.01*
Wound	0.21 *0.07*	ND	0.17 *0.05*	ND	0.11 *0.01*	0.13 *0.02*

N = 2 due to one misinjected animal.

Table S1: Biodistribution. Biodistribution of **[^{18}F]STX** in SNI rats sacrificed at specified time points post-injection (%ID/g, standard deviation below in italics, *n* = 3 per group)

SUPPLEMENTARY DISCUSSION

In order to demonstrate the specificity of the observed uptake, we attempted to block radiotracer binding by co-injection with an excess of **[^{19}F]STX**. However, the toxicity of the compound limited the amount that could be safely injected into a 300-350 g rat to ~9 µg. Upon co-injection of ~500 µCi of **[^{18}F]STX** with 9 µg of **[^{19}F]STX**, which corresponded to a 11-18-fold mass excess at the time of injection and is below the standard 100-fold minimum quantity typically employed for pre-blocking experiments, the signal from the neuroma in blocked animals was only modestly attenuated compared to unblocked animals ($p>0.05$, Supporting Figure 8). In order to reach the desired 100-fold excess and stay within the necessary toxicity window, one would need to substantially improve the specific activity of the radiotracer, a challenging task considering the number of steps involved in the current radiosynthesis of the tracer. However, the ability of **[^{19}F]STX** to block peak Na^+ current *in vitro* supports binding of the radiotracer to Na_Vs *in vivo*. Future studies are directed toward the development of alternative STX-based radiotracers that can prepared with higher specific activities.

REFERENCES

1. L. E. Llewellyn, *Nat. Prod. Rep.* **2006**, *23*, 200-222.
2. B. M. Andresen, J. Du Bois, *J. Am. Chem. Soc*. **2009**, *131*, 12524-12525.
3. E. Bennett, M. S. Urcan, S. S. Tinkle, A. G. Koszowski, S. R. Levinson, *J. Gen. Physiol*. **1997**, *109*, 327-343.
4. W. Song, Y. Xiao, H. Chen, N. M. Ashpole, A. D. Piekarz, P. Ma, A. Hudmon, T. R. Cummins, W. Shou, *J. Physiol.* **2012**, *590*, 5123-5139.
5. A. E. Ondrus, H. D. Lee, S. Iwanaga, W. H. Parsons, B. M. Andresen, W. E. Moerner, J. Du Bois, *Chem. Biol*. **2012**, *19*, 902-912.
6. O. Moran, A. Piccolo, F. Conti, *Biophys. J.* **2003**, *84*, 2999-3006.
7. G. D'Arcangelo, K. Paradiso, D. Shepherd, P. Brehm, S. Halegoua, G. Mandel, *J. Cell Biol*. **1993**, *122*, 915–921.
8. S. Guhlke, H. H. Coenen, G. Stoecklin, *Appl. Rad. Isotop.* **1994**, *6*, 715-727.
9. G. Tang, W. Zeng, M. Yu, M. Kabalka, *J. Label. Compd. Radiopharm.* **2008**, *51*, 68-71.
10. I. Decosterd, C. J. Woolf, *Pain* **2000**, *87*, 149–58.
11. C. A. Schneider, W. S. Rasband, K. W. Eliceiri, *Nat. Meth*. **2012**, *9*, 671-675.